Journal of Biomedical Optics

BiomedicalOptics.SPIEDigitalLibrary.org

Additivity of light-scattering patterns of aggregated biological particles

Alexander E. Moskalensky
Dmitry I. Strokotov
Andrei V. Chernyshev
Valeri P. Maltsev
Maxim A. Yurkin

SPIE.

Additivity of light-scattering patterns of aggregated biological particles

Alexander E. Moskalensky,[a,b] Dmitry I. Strokotov,[a,b] Andrei V. Chernyshev,[a,b] Valeri P. Maltsev,[a,b,c] and Maxim A. Yurkin[a,b,*]
[a]Institute of Chemical Kinetics and Combustion SB RAS, Institutskaya 3, Novosibirsk 630090, Russia
[b]Novosibirsk State University, Pirogova 2, Novosibirsk 630090, Russia
[c]Novosibirsk State Medical University, Krasny Prospect 52, Novosibirsk 630091, Russia

Abstract. The paper is focused on light scattering by aggregates of optically soft particles with a size larger than the wavelength, in particular, blood platelets. We conducted a systematic simulation of light scattering by dimers and larger aggregates of blood platelets, each modeled as oblate spheroids, using the discrete dipole approximation. Two-dimensional (2-D) light scattering patterns (LSPs) and internal fields showed that the multiple scattering between constituent particles can be neglected. Additionally, we derived conditions of the scattering angle and orientation of the dimer, under which the averaging of the 2-D LSPs over the azimuthal scattering angle washes out interference in the far field, resulting in averaged LSPs of the aggregate being equal to the sum of that for its constituents. We verified theoretical conclusions using the averaged LSPs of blood platelets measured with the scanning flow cytometer (SFC). Moreover, we obtained similar results for a model system of aggregates of polystyrene beads, studied both experimentally and theoretically. Finally, we discussed the potential of discriminating platelet aggregates from monomers using the SFC. [DOI: 10.1117/1.JBO.19.8.085004]

Keywords: light scattering; aggregates; platelets; scanning flow cytometer.

Paper 140295R received May 11, 2014; revised manuscript received Jun. 24, 2014; accepted for publication Jun. 30, 2014; published online Aug. 7, 2014.

1 Introduction

Scattering of light by particles is the basis of many approaches to study disperse systems, including aerosols, cosmic dust, biological samples, and so on. The most precise characterization of such systems is achieved by single-particle techniques, e.g., flow cytometry for biological cells[1] and spatial scattering measurement for airborne particles.[2] The characteristics of particles can be accurately determined when the particle geometry is relatively simple. In particular, this has been done with the scanning flow cytometer (SFC)[3,4] for such geometries as sphere, layered sphere, oblate spheroid, dimer of spheres, and capped cylinder, which are suitable optical models for many biological cells.[5–7] Scattering of light by particles with complicated geometry is more difficult to interpret, mainly due to a larger number of characteristics. The same applies to aggregates of simple particles which often occur in nature. For instance, the coagulation of emerging particles in a hydrocarbon flame is the key process of soot formation,[8] the adhesion of the related cells is a primary feature of the architecture of many tissues,[9] and aggregation of blood platelets is a process that stops bleeding, but may also cause thrombosis.[10]

The complexity of light scattering by aggregates comes from interaction of its constituent particles due to both multiple scattering (one particle modifying the field incident at another) and interference in the far field. The latter can be easily evaluated if the fields scattered by each particle (so-called partial fields) are known. By contrast, accounting for multiple scattering generally requires rigorous numerical methods. They may either explicitly consider the interaction of monomers,[11] as in the superposition T-matrix method,[12–14] or treat aggregates as a single particle, as in the discrete dipole approximation (DDA)[15] and the finite difference time-domain method.[16] As a specific case of superposition methods, one can consider the order-of-scattering solution, where the interaction between particles is iteratively considered.[17,18] It has a simple physical interpretation, but is not guaranteed to converge for an arbitrary system.

In many cases, partial fields can be accurately estimated, neglecting the multiple scattering. The simplest example of such an approximation is the Rayleigh-Gans-Debye (RGD) approximation applied to a whole cluster, which is equivalent to neglecting the multiple scattering not only between different particles but also between different parts of the same particle. RGD gives good precision for aggregates of nanoparticles even if the overall size of the cluster is larger than the wavelength.[19,20] The necessary requirement is that individual particles are small enough and the fractal dimension of the cluster is less than two.[21] When the particle size (more specifically, its phase-shift parameter[21]) increases, RGD becomes inapplicable even for individual particles, requiring rigorous techniques to compute the partial fields. More generally, neglecting multiple scattering leads to single-scattering approximation (SSA), called the first order of scattering. It is also called an independent scattering approximation (ISA),[22] but this term is usually applied to suspension of particles, in which relative position randomly varies over the time of measurement, or to aggregates in random orientation. In both cases, the far-field interference is also smoothed out; therefore, the final result is just a sum of that for the individual particles. We assign the latter definition to the term ISA to distinguish it from SSA.

*Address all correspondence to: Maxim A. Yurkin, E-mail: yurkin@gmail.com

0091-3286/2014/$25.00 © 2014 SPIE

The motivation of the present work is the characterization of biological cells aggregates by the SFC. For instance, the problem of separation of blood platelets from their aggregates based on the measured data is still not solved. This being done, one can trace the first stage of platelets' aggregation and determine the fundamental platelet-platelet binding constants and other characteristics of a patient's platelet function. In general, such a characterization implies two particular conditions. First, biological cells have a small refractive index relative to the medium, e.g., the typical values for *E. Coli* bacteria, red blood cells, and platelets are from 1.02 to 1.06.[7,23,24] However, their size is several times larger than the wavelength of visible light and the shape is nonspherical, which implies that RGD is generally not valid and a rigorous method, such as DDA,[25,26] is required. To the best of our knowledge, scattering by aggregates of nonspherical optically soft particles has not been rigorously simulated. However, it has been hypothesized[22] that both the large size and a small refractive index should decrease the importance of multiple scatterings, even when individual particles are situated close to each other. Second, the SFC measures the scattered intensity averaged over the azimuthal scattering angle as a function of polar angle – the so-called one dimensional (1-D) light scattering pattern (LSP).[4] Apart from leading to specific symmetries,[27] the averaging process (from 2-D to 1-D LSP) has the potential for smoothing out the interference similar to orientation averaging.

The goal of this paper is to analyze the validity of the SSA for aggregates of large optically soft particles, and to study the effect of the azimuthal angle averaging on the far-field interference. For that we rigorously simulate light scattering by aggregates of up to eight platelets and by dimers of polystyrene spheres, analyzing both 1-D and 2-D LSPs, as well as internal fields. Under the validity of the SSA, we derive additional conditions, which imply the additivity of 1-D LSPs of individual particles in the aggregate, i.e., the validity of ISA for 1-D LSPs. Those theoretical simulations and their conclusions are illustrated by experimental LSPs measured with the SFC. Finally, we discuss the consequences of this work for the development of characterization methods of platelet aggregates.

2 Theoretical Background

2.1 *Single-Sattering Approximation for Nonspherical Particles*

Scattering by an ensemble, or cluster, of N particles can be represented as the superposition of fields scattered by each particle, hereafter referred to as partial fields

$$\mathbf{E}^{\mathrm{sca}} = \sum_{k=1}^{N} \mathbf{E}_k^{\mathrm{sca}}. \tag{1}$$

The partial field of each sphere is, in turn, excited by the incident field and partial fields of other spheres

$$\mathbf{E}_k^{\mathrm{ex}} = \mathbf{E}^{\mathrm{inc}} + \left(\sum_{l \neq k} \mathbf{E}_l^{\mathrm{sca}} \right), \tag{2}$$

and is linearly related to this exciting field through a mapping T:

$$\mathbf{E}_k^{\mathrm{sca}} = \mathsf{T}(\mathbf{E}_k^{\mathrm{ex}}). \tag{3}$$

The essence of the SSA is the substitution of $\mathbf{E}^{\mathrm{inc}}$ instead of $\mathbf{E}^{\mathrm{ex}}$ into Eq. (3). The operator T, however, remains unchanged. Therefore, the first step of the SSA is to separately calculate the light scattering by each particle using exact techniques, such as the DDA or T-matrix approach. The second step is to combine the results using Eq. (1).

In the far-field region, where waves from individual particles are transverse and travel in the same direction, it is straightforward to compute the vector sum in Eq. (1). However, it is necessary to account for phase differences between partial waves. Let us consider a cluster of two particles, as shown in Fig. 1. The incident wave with wavenumber k travels along the z-axis, and orientation of the dimer is determined by angles (α and β), which are polar and azimuthal angles of the axis of symmetry of dimer p. The distance between the centers of spheres is d. The phase shift between two partial waves in the direction (θ and φ) is as follows:

$$\Delta(\theta, \varphi) = kd[\cos\,\beta\,\cos\,\theta + \sin\,\beta\,\sin\,\theta\,\cos(\alpha - \varphi)]. \tag{4}$$

Hereinafter, we consider $\alpha = 0$ without a loss of generality. Thus, under the SSA, the scattered field is given as

$$\mathbf{E}^{\mathrm{sca}} = \mathbf{E}_1^{\mathrm{sca}} + \mathbf{E}_2^{\mathrm{sca}} e^{\mathrm{i}\Delta}, \tag{5}$$

which is also valid for any element of the amplitude scattering matrix S.[28] The measured intensity is

$$\begin{aligned} I(\theta, \varphi) &= |\mathbf{E}^{\mathrm{sca}}|^2 = I_1 + I_2 + \mathbf{E}_1^{\mathrm{sca}} \cdot \overline{\mathbf{E}_2^{\mathrm{sca}} e^{\mathrm{i}\Delta}} + \overline{\mathbf{E}_1^{\mathrm{sca}}} \cdot \mathbf{E}_2^{\mathrm{sca}} e^{\mathrm{i}\Delta} \\ &= I_1 + I_2 + 2\mathrm{Re}[\mathbf{E}_1^{\mathrm{sca}} \cdot \overline{\mathbf{E}_2^{\mathrm{sca}} e^{\mathrm{i}\Delta}}], \end{aligned} \tag{6}$$

where I_1 and I_2 are the intensities of the first and second monomers in the absence of another one, respectively, and the bar denotes the complex conjugation. The last term corresponds to the interference of the waves scattered by each particle.

Further, we only consider the case when intensity is given by the S_{11} element of the Mueller matrix [compare Eq. (12)], omitting the factor $1/(kr)^2$ (Ref. 28). This intensity is obtained analogously to Eqs. (5) and (6):

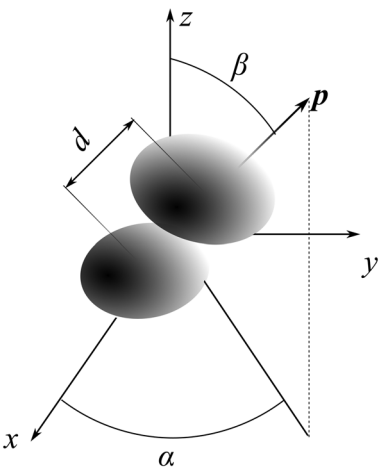

Fig. 1 The layout of light-scattering problem for a cluster of two particles.

$$I(\theta,\varphi) = S_{11} = S_{11}^{(1)} + S_{11}^{(2)} + \mathrm{Re}[f(\theta,\varphi)e^{-\mathrm{i}\Delta}],$$
$$f(\theta,\varphi) \equiv S_1^{(1)}\overline{S_1^{(2)}} + S_2^{(1)}\overline{S_2^{(2)}} + S_3^{(1)}\overline{S_3^{(2)}} + S_4^{(1)}\overline{S_4^{(2)}}, \quad (7)$$

where the superscripts denote the number of the particle and the left-hand side is the value for the aggregate. We used Eq. (7) for evaluation of $I(\theta,\varphi)$ for dimers of blood platelets (see Sec. 4.3) and its simplified form in Eq. (8) for polystyrene beads (see Sec. 4.1).

2.2 *Effect of Integration over Azimuthal Angle*

In this section, we will consider the effects of integration over φ under the assumption of single scattering. Let us first consider a particular case of a cluster of two identical spheres. In this case, Eq. (7) can be simplified as follows:

$$I(\theta,\varphi) = 2S_{11}^{(1)}(\theta)\{1 + \cos[\Delta(\theta,\varphi)]\}, \quad (8)$$

which can be easily integrated over φ:

$$I(\theta) = \frac{1}{2\pi}\int_0^{2\pi} S_{11}(\theta,\varphi)\mathrm{d}\varphi = 2S_{11}^{(1)}(\theta)\left\{1 + \frac{1}{2\pi}\int_0^{2\pi}\cos[\Delta(\theta,\varphi)]\mathrm{d}\varphi\right\}. \quad (9)$$

The latter integral is equal to

$$\int_0^{2\pi}\cos[\Delta(\theta,\varphi)]\mathrm{d}\varphi = \cos\tau\int_0^{2\pi}\cos(\rho\cos\varphi)\mathrm{d}\varphi = 2\pi\cos(\tau)J_0(\rho),$$
$$\tau \equiv kd\cos\beta\cos\theta,$$
$$\rho \equiv kd\sin\beta\sin\theta, \quad (10)$$

where J_0 is the Bessel function of the zeroth order. The function (10) takes the value of order unity in a special case when the argument of Bessel function $\rho = 0$ and is much smaller when $\rho \gg 1$. Particularly, when $kd \gg 1$ and both β and θ are not close to 0 or π, the majorant of Eq. (10) has asymptotic behavior $\rho^{-1/2}$. This means that the interference of partial waves is washed out by integration over φ for dimers of spherical particles, i.e., the ISA is valid. The mathematical fact that ISA is not valid for $\theta = 0$ or π corresponds to such physical phenomena as diffraction (forward-scattering interference) and coherent backscattering.[22]

In the general case of a cluster of two different nonspherical particles, the simple expression (9) takes a more complex form

$$I(\theta) = I_1(\theta) + I_2(\theta) + 2\,\mathrm{Re}[\exp(-\mathrm{i}\tau)\int_0^{2\pi} f(\theta,\varphi)\exp(-\mathrm{i}\rho\cos\varphi)\mathrm{d}\varphi]. \quad (11)$$

The cross-term (function f) now depends on φ and cannot be taken outside the integral in Eq. (11). However, if this dependence is slower than the oscillations of the exponent (characteristic scale of the dependence is much larger than $\rho^{-1/2}$), it can be shown by the stationary phase method that the integral has the same asymptotic behavior $\rho^{-1/2}$ and, therefore, the ISA is also valid. Finally, other elements of the Mueller matrix satisfy relations, similar to Eqs. (7) and (11), but with a different function f (always a quadratic function of the amplitude matrix elements).

3 Methods

3.1 *Scanning Flow Cytometer*

The SFC is a device that measures 1-D LSPs of individual particles in a flow. Technical features of the SFC were previously described in detail elsewhere.[3] In short, the scattering is measured as a particle moves along the optical axis of a semi-spherical mirror. The measurement time of one particle is about 1 ms, which allows one to neglect particle rotation during the measurement. The measured LSP is expressed as

$$I(\theta) = \frac{1}{2\pi}\int_0^{2\pi}[S_{11}(\theta,\varphi) + S_{14}(\theta,\varphi)]\mathrm{d}\varphi. \quad (12)$$

Note that the second term vanishes after integration over φ for particles having a symmetrical plane[29] and is typically much smaller than the first term for other particles. In particular, its contribution to $I(\theta)$ is estimated to be at most 0.1% for all considered aggregates. Therefore, we limit ourselves to the consideration of the S_{11} element, both in 1-D [Eq. (12)] and 2-D LSPs. The specific SFC was fabricated by Cytonova Ltd. (Novosibirsk, Russia). It is equipped with a 20-mW laser of 488 nm (Sapphire 488-20 CDRH, Coherent, California) wavelength for generation of the LSPs of individual particles. Another 40-mW laser of 660 nm (LM-660-20-S) wavelength is used for generating a trigger signal. The measurement range of θ is from 10 to 60 deg.

3.2 *Sample Preparation*

Polystyrene beads were used for the device alignment and calibration. We also used FluoSpheres® F-8823 beads (diameter 1.1 μm, Life Technologies, New York), labeled by fluorescein isothiocyanate, for the measurement of LSPs of beads aggregates. The aggregates of beads were spontaneously formed in suspension.

For the study of blood platelet aggregates, human blood was taken from a healthy donor by venipuncture and collected in a BD Vacutainer® tube containing sodium citrate. Platelet plasma was obtained by sedimentation for 1 h at room temperature. The aggregation of platelets was initiated by the addition of adenosine diphosphate at a final concentration of 20 μM. At certain moments after the initiation (1 and 15 min), part of the platelet plasma was 200-fold diluted and measured with the SFC (see Sec. 3.1).

3.3 *Light-Scattering Codes*

We used a multiple sphere T-matrix (MSTM) code[30] to simulate light scattering by aggregates of spherical particles. We slightly modified the code to calculate the 2-D LSPs. These simulations were done for a polar scattering angle from 10 to 60 deg corresponding to the operational range of the SFC. To simulate light scattering by aggregates of nonspherical platelets, we used the DDA code ADDA v1.1.[31] The 1-D LSPs were simulated for the full range of θ (0 to 180 deg) with the integration over φ from 0 to 360 deg in 32 steps. In several cases, we also calculated 2-D LSPs and internal fields. The results of the SSA for aggregates were obtained by a separate code, which combines

Table 1 Parameter ranges of activated platelets. Relative (to water) refractive index is given in parentheses.

Parameter	Lower boundary	Upper boundary
r_{ev}	1.1 μm	1.3 μm
ε	1	2
n	1.37 (1.024)	1.39 (1.040)
β	0 deg	90 deg

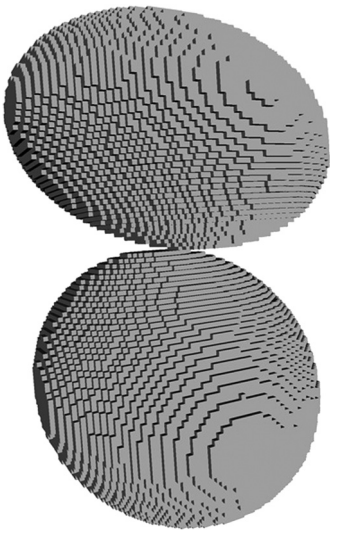

Fig. 2 The example of constructed dipole configuration for simulation of dimer blood platelets. Visualized with LiteBil.[36]

the corresponding results for spherical or nonspherical monomers according to Eqs. (8) or (7), respectively.

3.4 *Optical Model of Platelets and Their Aggregates*

Unlike polystyrene beads, blood platelets are essentially heterogeneous in size and shape because they are originally cell fragments.[32,33] In a normal state, platelets have a discoid shape with an aspect ratio of 2–8 and a volume of 2–30 fL.[34,35] Activated by a physical or chemical stimulus, platelets change their shape and membrane receptors and become capable of aggregation with each other. The shape of the activated platelet is more spherical (aspect ratio 1–2), and membrane outgrowths (pseudopodia) are present. However, modeling both resting and activated platelets as oblate spheroids for computing light scattering is reasonable.[7]

To construct an aggregate, we first specified two oblate spheroids corresponding to activated platelets. Their parameters r_{ev} (equi-volume sphere radius), ε (aspect ratio), n (refractive index), and β were randomly chosen from physiological ranges (Table 1). We discretized each spheroid into a set of dipoles, providing at least 12 dipoles (discretization element in the DDA) both on the wavelength and on the thickness of the spheroid. Then, a random rotation around the z-axis was applied to the second spheroid, and it was translated along the positive direction of the z-axis, until two sets of dipoles stopped overlapping. An example of the resulting dipoles configuration is shown in Fig. 2. Finally, we randomly set the Euler angles of the dimer orientation with respect to the incident wave. A similar procedure was used to construct larger aggregates by the consecutive addition of single spheroids.

4 Experiments and Simulations

4.1 *Dimers of Polystyrene Beads*

The SFC measures fluorescence intensity simultaneously with the LSP. Thus, monomers and dimers of fluorescent microspheres (see Sec. 3.2) can be easily separated based on their fluorescence signals. The geometrical layout of a dimer in the SFC is shown in Fig. 1. In Fig. 3(a), several typical experimental

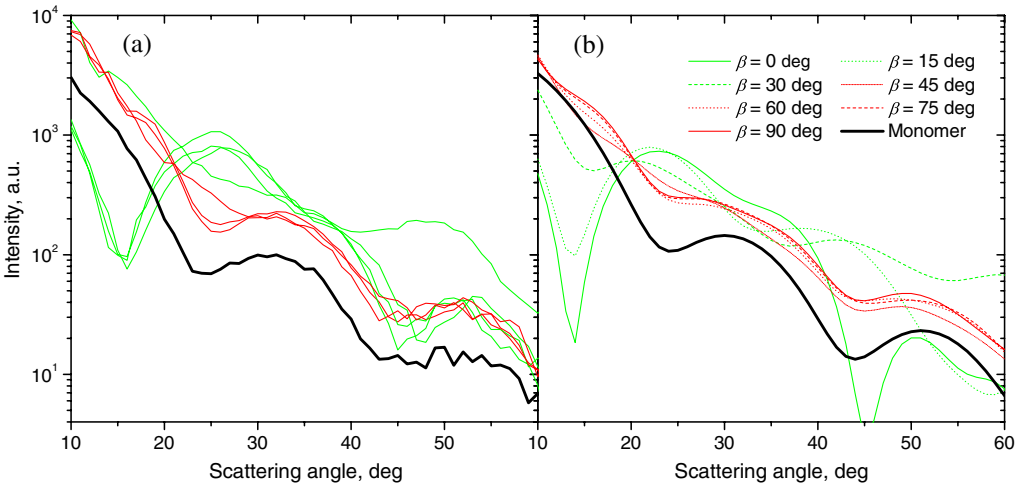

Fig. 3 Light scattering patterns (LSPs) of dimers of polystyrene beads measured with the SFC (a, thin lines) and calculated with the multiple sphere T-matrix (MSTM) for different orientations of dimers (b, thin lines). LSPs of monomers are shown in each graph (thick line). Red lines in (a) correspond to approximately independent scattering of monomers in dimers.

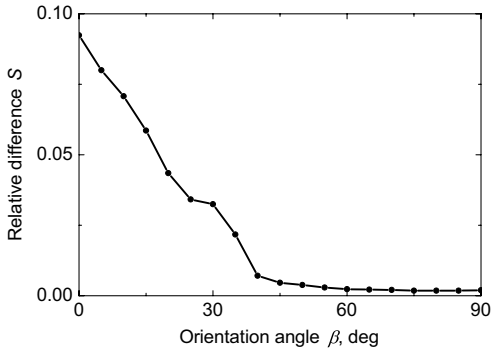

Fig. 4 The relative difference between LSP of dimer and doubled LSP of monomer versus the orientation angle β.

LSPs of dimers are shown together with a typical LSP of a single bead. One can see that some of them, highlighted in red in Fig. 3(a), have approximately the same shape as the LSP of the single bead but with the double intensity.

Numerical simulations of LSPs of bispheres (two touching spheres) show the same types of LSPs, see Fig. 3(b). The thick line is an LSP for a single sphere with diameter of 1.1 μm and refractive index of 1.605 (1.20 relative to the water) calculated with the Mie theory. Thinner lines are LSPs for the dimer of such spheres as calculated with the MSTM, as described in Sec. 3.3. The specific observed LSPs of dimers, equal to double that of monomers, correspond to an orientation angle β from 50 to 90 deg. The simulations are slightly different from the experiment (e.g., in forward scattering), which can be related to a possible gap between real beads, slightly different sizes, or other deviations from the model. However, the effect of convergence of the dimer LSP to the double LSP of a monomer with increasing angle β is clearly visible. We define the following relative difference S (in logarithmic scale) to quantify this convergence

$$S = \frac{\sum_i [\log I(\theta_i) - \log I_{\text{sum}}(\theta_i)]^2}{\sum_i [\log I_{\text{sum}}(\theta_i)]^2}, \tag{13}$$

where $I(\theta)$ is the LSP of dimer, $I_{\text{sum}}(\theta)$ is the sum of LSPs of monomers that constitute it, and summation is over the scattering angles θ_i where the LSPs are calculated. The dependence of S on β is shown in Fig. 4, quantitatively supporting the above conclusions.

Let us also consider 2-D LSPs. For a single sphere, it is independent of φ. This is substantially different for a bisphere with an orientation angle near 90 deg, in which 2-D LSPs show oscillations along φ [Fig. 5(a)]. These oscillations are due to the interference of partial waves (see Sec. 2.2), which is confirmed by the fact that the SSA [Eq. (8)] results in almost the same 2-D LSP [Fig. 5(d)]. The dimer with $\beta = 50$ deg is, in some sense, a critical point (Fig. 4), where the exact and approximate results are still close to each other [Figs. 5(b) and 5(e)]. In contrast, for $\beta = 10$ deg, the 2-D LSP for the SSA only remotely resembles the exact one [Figs. 5(c) and 5(f)].

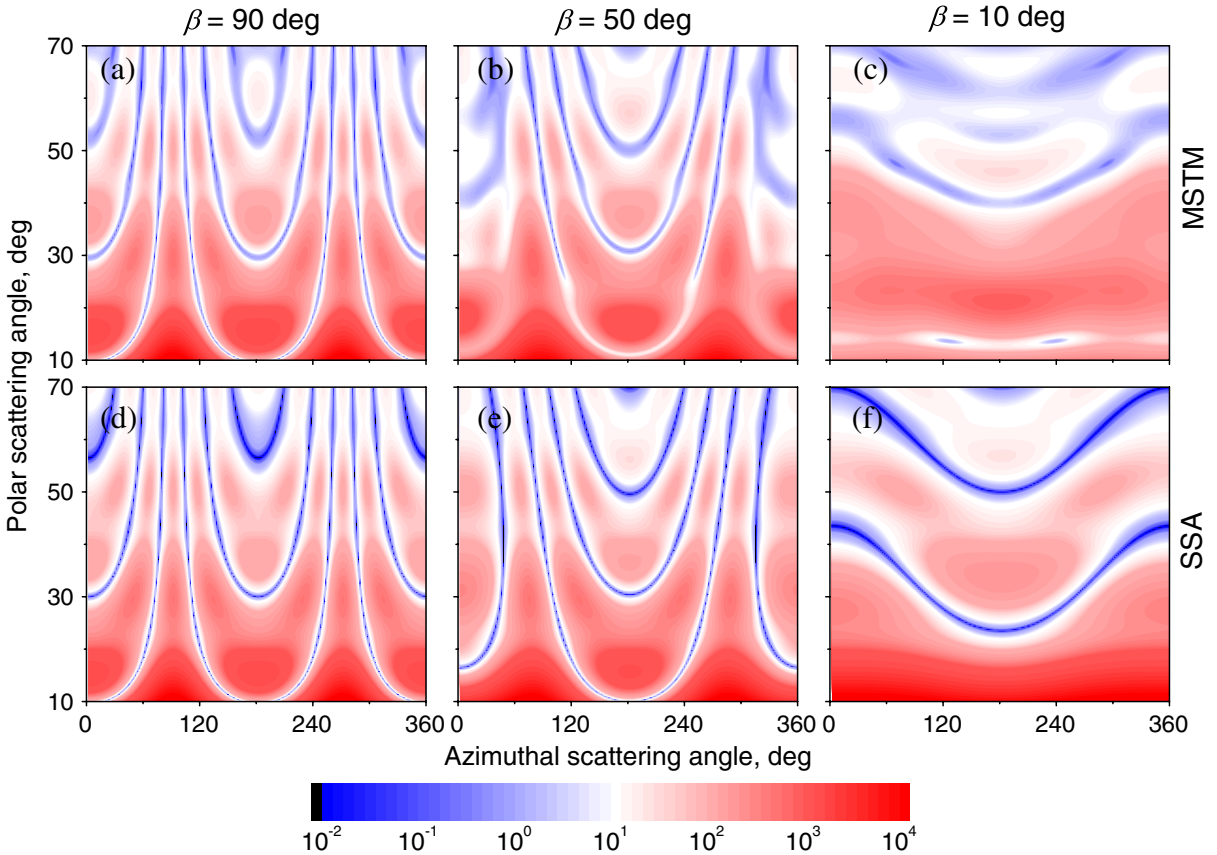

Fig. 5 Two-dimensional (2-D) LSPs of dimers of polystyrene beads—MSTM simulations (a–c) and the SSA (d–f) for $\beta = 90$, 50, and 10 deg respectively.

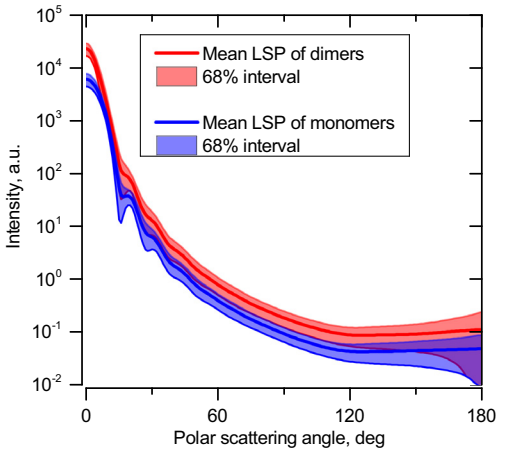

Fig. 6 Mean LSPs of platelets dimers and monomers. Also intervals corresponding to 68% probability are shown.

Therefore, multiple scattering is significant only when one sphere is shadowing another. It is nonobvious that the multiple scattering is not significant in the dimer of polystyrene beads down to $\beta = 45$ deg, despite the relatively large refractive index. The ISA for 1-D LSPs is valid (except for the near-forward direction) whenever the SSA is valid, i.e., they are additive in agreement with the analysis in Sec. 2.

4.2 *Dimers of Blood Platelets*

We constructed 8756 platelet dimers as described in Sec. 3.4. The LSPs of both dimer and constituent monomers were simulated with the DDA as described in Sec. 3.3. The mean LSPs for dimers and single spheroids are shown in Fig. 6. It should be noted that the mean LSPs are almost identical except for overall intensity and perhaps forward scattering (0 to 5 deg). The same fact is observed if one replaces all the LSPs of the spheroids with an independently calculated set. Thus, the mean LSP of the dimer is the double mean LSP of the spheroid, i.e., the ISA is valid on average.

Further, we tested the validity of the ISA for single aggregates. The measure of difference S [Eq. (13)] is plotted versus β in Fig. 7. Direct comparison with Fig. 4 is not completely adequate due to the different range of angles for LSPs; however, calculating S in a limited range of scattering angles (the same as for polystyrene beads) qualitatively results in the same picture as Fig. 7. Although the graph is noisy due to the variability of considered platelets, the general trend is the same as in Fig. 4.

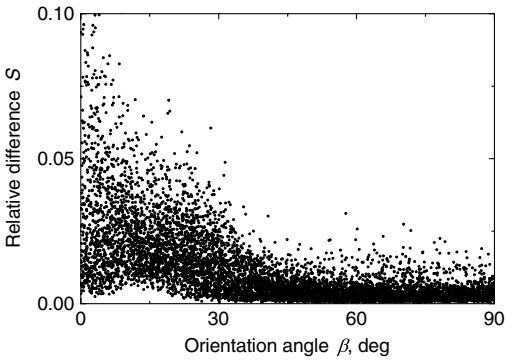

Fig. 7 The relative difference between LSP of dimer and sum of LSPs of its constituents versus the orientation angle β.

Moreover, there are points with a small S even for a small β. This can be explained by a smaller value of the refractive index of platelets compared to that of the polystyrene beads.

The vast majority of dimers (88%) have a value of S smaller than 0.025, and the fraction is even larger (99.9%) for $\beta > 40$ deg. It is important to understand how good the qualitative agreement is between LSPs corresponding to this value of S. We provide some examples below in Fig. 8. Figure 8(a) corresponds to one of the worst differences, found in the left-top corner in Fig. 7. In this case, LSPs are visually different, i.e., multiple scattering and/or interference results in noticeable distortion of the LSP. However, in Fig. 8(b) another dimer with the same orientation has $S < 0.025$. Still not coinciding perfectly, the curves have the same structure except for forward- and back-scattering, indicating the validity of the ISA, as discussed in Sec. 2. The same can be said for Figs. 8(c) and 8(e), corresponding to intermediate and large β, respectively, although the visual agreement is even better. The vast majority of other dimers have a smaller value of S and hence better agreement should be expected. For instance, Figs. 8(d) and 8(f) represent one of the best fulfillments of the ISA (the smallest values of S).

4.3 *Two-Dimensional Light Scattering Patterns and Internal Fields of Platelets Aggregates*

The LSPs shown in Fig. 8 indicate the validity of the ISA and, indirectly, the validity of the SSA. To test the latter directly, we examined 2-D LSPs – they are shown for a single dimer in different orientations in Fig. 9. They are very similar, including intensity and oscillatory structure, although the agreement gets slightly worse with a decreasing β.

To better understand the applicability of the SSA, we examined the internal fields for the same dimer. The magnitude (squared norm) of internal field in the xz-plane for the perpendicular polarization of the incident field is shown in Fig. 10. When the SSA is valid, the fields of each monomer in the dimer should be identical to that of the monomer. This is always so for the first (lower) monomer, but for the second one it is approximately accomplished only for $\beta = 90$ deg. The discrepancy of internal fields for $\beta = 50$ deg is in the region that is shadowed (or focused upon) by the first particle. The same applies to the case of $\beta = 10$ deg, although there is some discrepancy in the nonshadowed region as well. It is important to note that Fig. 10 only shows the central section, which is expected to have the strongest distortions of the internal fields. In other sections, where the distance between monomers is larger, internal fields are almost unchanged compared to that of single particles. Therefore, the fraction of platelet volume where internal fields are different is rather small. This explains the good agreement of 2-D LSPs (Fig. 9). Thus, we expect the validity of SSA for aggregates of optically soft particles, especially when the area of contact is relatively small. For particles with a large contiguity, multiple scattering should be significant. For instance, if we virtually separated a spheroid into two halves, the 1-D LSPs of the halves would not be additive. The same is expected for internal aggregation, i.e., one particle inside another.

Note also that the amplitude of the internal fields is significantly different from one even for the SSA, which indicates that the RGD (equivalent to assuming an internal field equal to the incident one) is not valid in this case. In other words, interaction (multiple scattering) between the different parts of the platelet is more significant than that between different platelets.

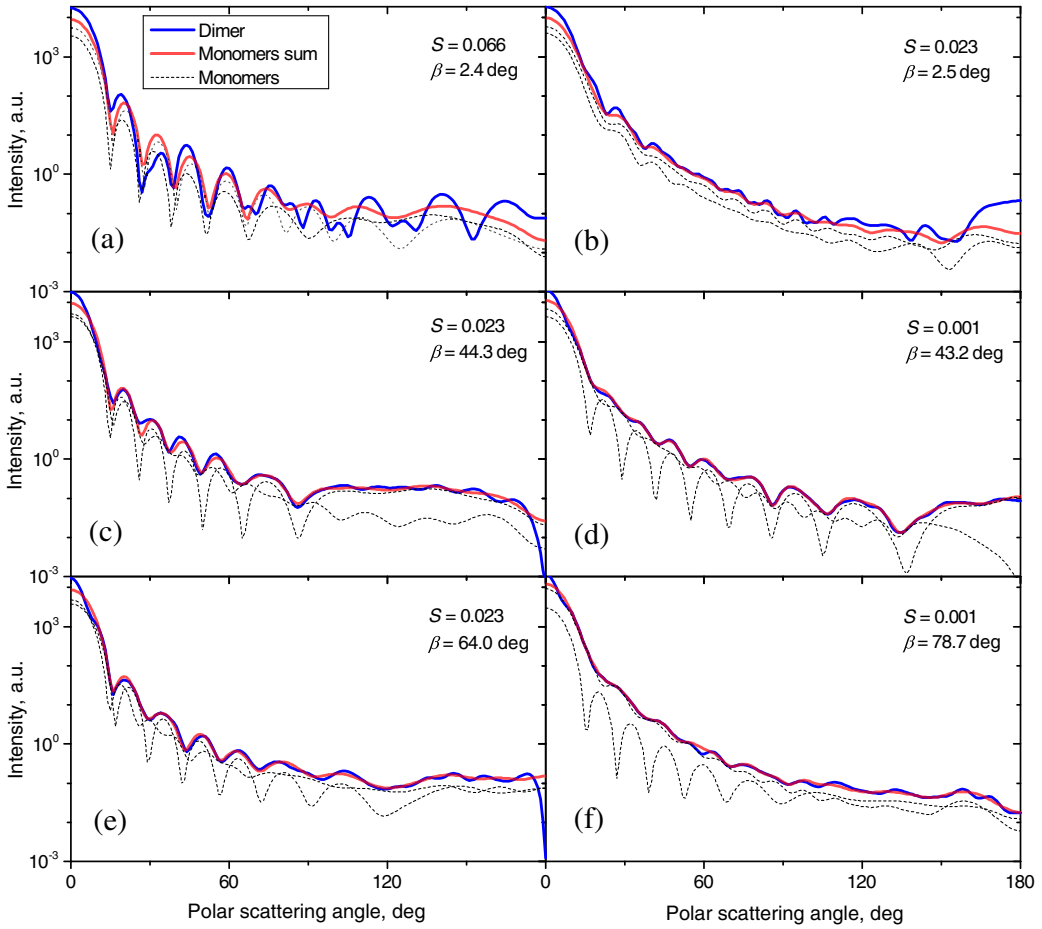

Fig. 8 Examples of LSPs of dimers and sum of LSPs of monomers (solid lines). The relative difference S and orientation angle β are shown in each plot. LSPs of monomers are shown as well (dashed lines). Left and right columns correspond to typical large and small values of S, respectively, among small (a, b), intermediate (c, d) and large (e, f) values of β.

Thus, we conclude that the SSA is almost always valid for platelet aggregates (at least for 2-D LSPs), even more than for polystyrene beads (Sec. 4.1). We hypothesize that the SSA can be a promising approximate method to simulate light scattering by an aggregate of biological particles. First, one should calculate the 2-D distributions of scattered electric fields, e.g., in the form of an amplitude scattering matrix,[28] for each component of the aggregate. Second, these 2-D LSPs should be combined using Eqs. (6) or (7). Potential acceleration depends on the used method and details of the aggregate. In our DDA simulations, there was almost no acceleration for dimers of blood platelets, and about 30% for octamers (see Sec. 4.4). However, drastic acceleration is expected for problems where the monomers can be treated by a simpler light scattering method. Consider, for instance, a platelet-leukocyte aggregate, which can be modeled as an oblate spheroid in contact with a larger two-layered sphere;[5] the Mie theory can be used for the latter. We stress, however, that applicability of the SSA to problems other than those considered in this paper should be tested separately.

4.4 *Larger Platelets Aggregates*

Several larger platelets aggregates were constructed as described in Sec. 3.4. Previously made shapes of dimers and monomers (see Sec. 4.2) were used for this purpose. In Fig. 11, the simulated LSPs for three aggregates are shown: planar and tetrahedral tetramers and octamers (see inset on each plot for particular geometries). The sums of LSPs of the monomers are also shown (gray lines). Surprisingly, the visual agreement is very good, although forward- and backscattering diverge as before (Fig. 8). Figure 11(b) is especially nontrivial: the upper monomer is strongly shadowed by lower ones, but multiple scattering still has little effect on the LSP.

This leads to two important implications. First, the LSP of the aggregate is, on average, proportional to the number of its monomers. However, since the overall magnitude of monomer LSPs is not constant due to the natural variability of blood platelets, this proportionality does not hold on a single-aggregate level. Second, the structure of the LSP of the aggregate, i.e., maximum and minimum, resembles that of the monomer, but can be smoothed out due to different locations of the maximum and minimum of LSP of the monomers. For instance, the LSP of the octamer [Fig. 11(c)] is apparently less (has a smaller amplitude of oscillations) than that of tetramers [Figs. 11(a) and 11(b)].

A similar effect is seen in experiments. The LSPs of platelet aggregates were measured with the SFC (Sec. 3.1) in different time points after the initiation of aggregation. In Fig. 12, the first 10 measured LSPs are shown for 1 and 15 min batches. One can see the growth of intensity and a decrease in the contrast of the

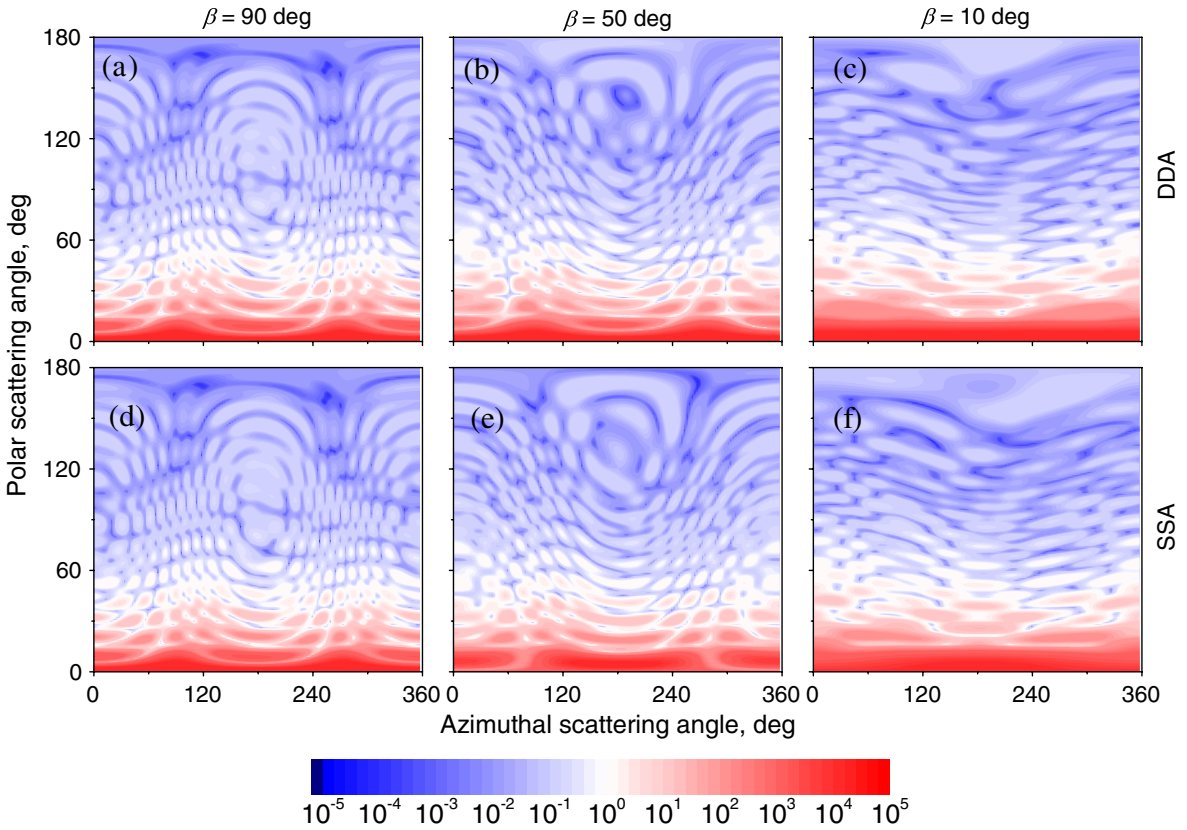

Fig. 9 2-D LSPs calculated with the DDA (a–c) and the SSA (d–f) for different orientation of the same dimer ($\beta = 90$, 50, and 10 deg, respectively).

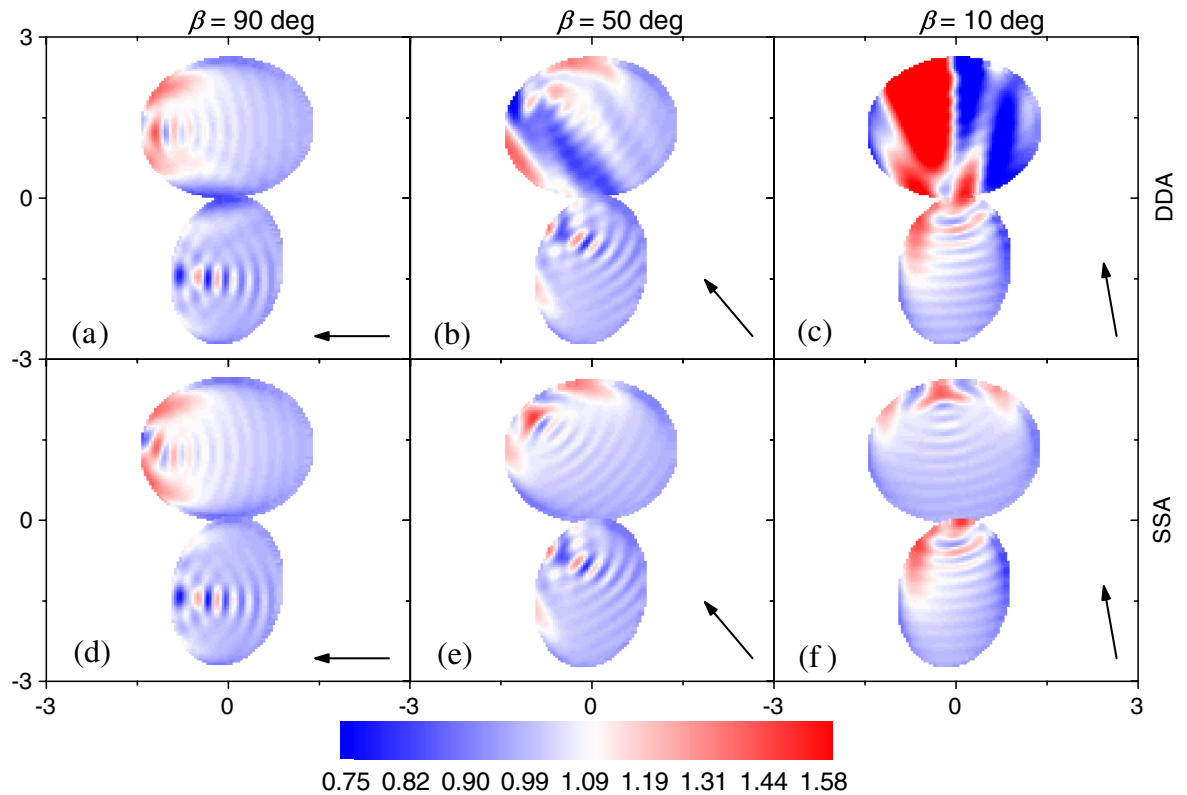

Fig. 10 Internal fields (squared norm) of dimers of blood platelets (a–c) and of single platelets that constitute it (d–f, shown together as in the aggregate) for different directions of propagation of the incident field (designated by arrows).

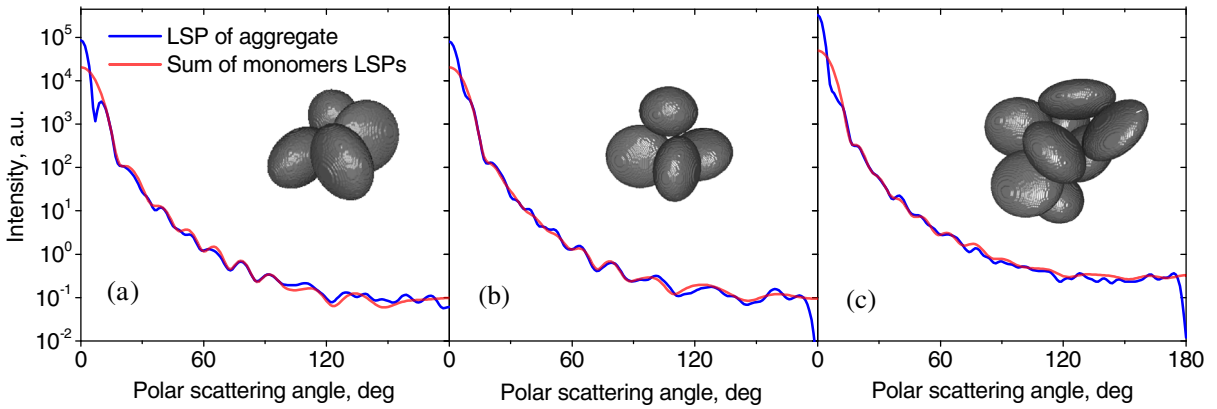

Fig. 11 Simulated LSPs and sum of LSPs of monomers for different aggregates: planar (a) and tetrahedral (b) tetramer and octamer (c). The incident wave propagates from below. Aggregates are visualized with LiteBil.[36]

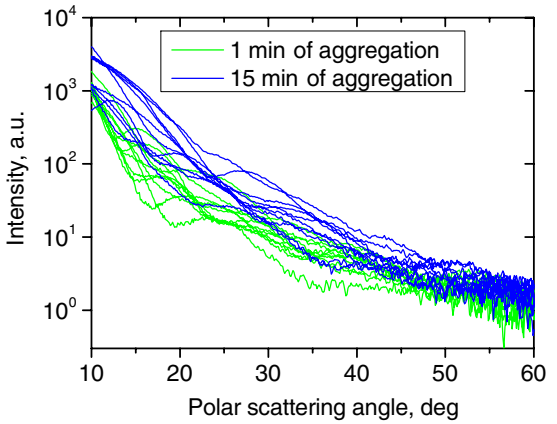

Fig. 12 Experimental LSPs 1 min (green lines) and 15 min (blue lines) after the initiation of aggregation. First 10 LSPs are shown in each case.

LSP, which can be used for separation of monomers from large aggregates. However, unambiguous separation of monomers from dimers seems impossible on this basis. That is unfortunate, since it is this very first step of aggregation that is important for determination of platelet-platelet binding constants.

4.5 *Separation of Monomers from Dimers*

The fact that the LSP of the dimer is close to the sum of the LSPs of its monomers has an important implication for the separation of monomers from dimers. Let us start with the simple case when the dimer consists of two identical spheroids. The structure of its LSP is the same as of the LSP of a spheroid and the intensity is two times larger. On the other hand, the intensity of the LSP of a single spheroid rises with the increasing refractive index approximately maintaining its structure. Thus, the LSP of the dimer can be very similar to the LSP of a single spheroid with a larger refractive index. The same reasoning applies to the case of a dimer consisting of different spheroids, at least when the spheroids are not greatly different. Then, one can expect a spheroid with average parameters and increased refractive index to have an LSP similar to that of the dimer.

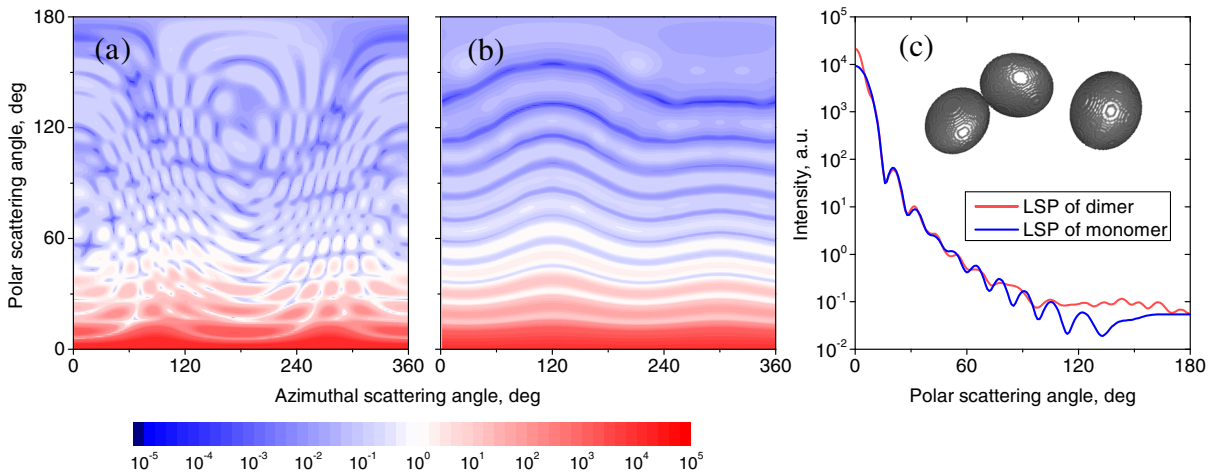

Fig. 13 LSPs for dimer and monomer: 2-D LSPs are apparently different—(a) and (b), respectively, while the LSPs averaged over φ agree well in forward hemisphere (c). Dimer and monomer are also shown on (c), refractive index of the latter is 1.035, while for monomers in dimer it is 1.028 and 1.031.

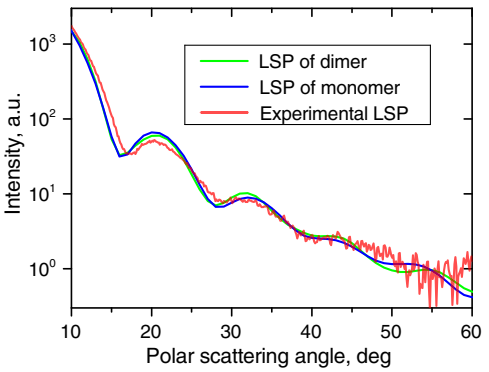

Fig. 14 Experimental LSP that agrees well both with LSP of dimer and with LSP of monomer that are the same as in Fig. 13(c).

A typical situation is shown in Fig. 13. 2-D LSPs of the dimer and the monomer are completely different, but coincide after averaging over φ. The LSP of the monomer is previously chosen as the nearest one from the constructed database of LSPs of single spheroids.[7] That database was constructed for scattering angles from 10 to 70 deg; therefore, the best agreement is seen in this range. However, the agreement at the near-forward direction is unlikely since it is largely determined by the overall size of the particle. The parameters of the monomer correspond to those of typical blood platelets. Moreover, such LSPs are actually measured in experiments (Fig. 14), and it is generally impossible to unambiguously attribute the measured LSP to that of the dimer or monomer.

Still the separation of monomers from dimers from light scattering is not hopeless. There are several promising ideas with which to do it. The first of these is the measurement of 2-D LSPs, which is possible with the modification of the SFC.[37] The 2-D LSPs are largely different for dimers and monomers. However, the effect of pseudopodia on the 2-D-LSP is still not understood, and they may potentially introduce a complex structure to the 2-D LSP of the monomer, similar to that of the dimer. The second way is the measurement of the very forward scattering (0 to 5 deg), which is complicated by the interference of scattered and incident waves. Another possibility is to reverse the incident laser beam in the SFC for measurement of the LSP in the backward hemisphere since, in a number of cases, we saw larger deviations at that scattering angle [Figs. 8(a), 8(b), and 13(c)]. However, this effect is probably not universal. Finally, in this paper, we analyzed only the intensity of the scattered light, leaving polarization as an interesting future topic of research. This is especially relevant since certain combinations of Mueller matrix elements can be measured with the SFC.[4]

5 Conclusion

On the basis of systematic numerical simulations, we showed that the SSA is valid for the vast majority of aggregates of blood platelets, and, in many cases, for aggregates of polystyrene beads. We hypothesize that such an approximation should also be valid for other aggregates with similar sizes (of several wavelength), relative refractive indices (close to unity), and sparsity (non-overlapping monomers with a small area of contact). This may significantly simplify the simulation of light scattering by such aggregates, especially when the monomers can be treated with simple simulation methods. However, the multiple scattering can only be neglected between the monomers, but not between the different parts of the monomer. Thus, simpler approximations, like the Rayleigh-Debye-Gans one, are generally inapplicable.

Averaging (integration) over the azimuthal scattering angle φ is shown to eliminate the interference of partial waves in the far field, except for near-forward or backward scattering angles or for dimers orientated along the incident direction. Thus, in many cases, the LSP of the aggregate integrated over φ is expressed by the simple sum of 1-D LSPs of its constituent particles. On the one hand, if monodisperse biological systems are considered, i.e., cells with a relatively narrow distribution of sizes, the additivity may help in quick counting the number of monomers in the aggregates based on the intensity of its 1-D LSP. On the other hand, this complicates the identification of aggregates since their LSPs retain the structure of monomers' LPSs, which was confirmed by measurements with the SFC.

The dependence of LSP on φ is completely different for monomers and other aggregates. This can be the basis for identification of aggregates of blood platelets. For instance, the SFC can be modified for measurement of either 2-D LSPs[37] or another signal related to dependence on φ. However, this requires extensive experimental work at the limit of modern technology sensitivity.

Acknowledgments

We thank two anonymous reviewers for helpful comments. The experimental work with the scanning flow cytometer was supported by Russian Foundation of Basic Research (Grant No. 12-04-00737-a), whereas Russian Science Foundation (14-15-00155) supported theoretical simulations. A.E.M., D.I.S., and M.A.Yu. also acknowledge the support by the Stipend of the President of Russian Federation for young scientists.

References

1. M. J. Fulwyler, "Electronic separation of biological cells by volume," *Science* **150**(3698), 910–911 (1965).
2. P. H. Kaye, "Spatial light-scattering analysis as a means of characterizing and classifying non-spherical particles," *Meas. Sci. Technol.* **9**(2), 141 (1998).
3. V. P. Maltsev, "Scanning flow cytometry for individual particle analysis," *Rev. Sci. Instrum.* **71**(1), 243–255 (2000).
4. D. I. Strokotov et al., "Polarized light-scattering profile–advanced characterization of nonspherical particles with scanning flow cytometry," *Cytometry A* **79A**(7), 570–579 (2011).
5. D. I. Strokotov et al., "Is there a difference between T- and B-lymphocyte morphology?," *J. Biomed. Opt.* **14**(6), 064036 (2009).
6. A. I. Konokhova et al., "Light-scattering flow cytometry for identification and characterization of blood microparticles," *J. Biomed. Opt.* **17**(5), 057006 (2012).
7. A. E. Moskalensky et al., "Accurate measurement of volume and shape of resting and activated blood platelets from light scattering," *J. Biomed. Opt.* **18**(1), 017001 (2013).
8. Ü. Ö. Köylü et al., "Fractal and projected structure properties of soot aggregates," *Combust. Flame* **100**(4), 621–633 (1995).
9. H. Lodish et al., Eds., *Molecular Cell Biology*, 5th Ed., W.H. Freeman, New York (2004).
10. A. D. Michelson, Ed., *Platelets*, 2nd ed., Academic Press, San Diego, CA (2006).
11. M. I. Mishchenko, D. W. Mackowski, and L. D. Travis, "Scattering of light by bispheres with touching and separated components," *Appl. Opt.* **34**(21), 4589–4599 (1995).
12. M. I. Mishchenko, L. D. Travis, and D. W. Mackowski, "T-matrix computations of light scattering by nonspherical particles: a review," *J. Quant. Spectrosc. Radiat. Transf.* **55**(5), 535–575 (1996).
13. Y. Xu, "Scattering Mueller matrix of an ensemble of variously shaped small particles," *J. Opt. Soc. Am. A* **20**(11), 2093–2105 (2003).

14. A. Doicu, T. Wreidt, and Y. Eremin, *Light Scattering by Systems of Particles–Null-Field Method with Discrete Sources: Theory and Programs*, Springer, Berlin (2006).
15. M. A. Yurkin and A. G. Hoekstra, "The discrete dipole approximation: an overview and recent developments," *J. Quant. Spectrosc. Radiat. Transf.* **106**(1–3), 558–589 (2007).
16. A. Taflove and S. C. Hagness, *Computational Electrodynamics: The Finite-Difference Time-Domain Method*, Artech House, Boston (2005).
17. D. W. Mackowski, "Analysis of radiative scattering for multiple sphere configurations," *Proc. R. Soc. Lond. Ser. Math. Phys. Sci.* **433**(1889), 599–614 (1991).
18. Y. Xu, "Electromagnetic scattering by an aggregate of spheres," *Appl. Opt.* **34**(21), 4573–4588 (1995).
19. M. Y. Lin et al., "Universality in colloid aggregation," *Nature* **339**(6223), 360–362 (1989).
20. G. Wang and C. M. Sorensen, "Experimental test of the Rayleigh-Debye-Gans theory for light scattering by fractal aggregates," *Appl. Opt.* **41**(22), 4645–4651 (2002).
21. C. M. Sorensen, "Light scattering by fractal aggregates: a review," *Aerosol Sci. Technol.* **35**(2), 648–687 (2001).
22. M. I. Mishchenko, L. D. Travis, and A. A. Lacis, *Scattering, Absorption, and Emission of Light by Small Particles*, Cambridge University Press, Cambridge, NY (2002).
23. A. I. Konokhova et al., "High-precision characterization of individual E. coli cell morphology by scanning flow cytometry," *Cytom. Part J. Int. Soc. Anal. Cytol.* **83**(6), 568–575 (2013).
24. D. H. Tycko et al., "Flow-cytometric light scattering measurement of red blood cell volume and hemoglobin concentration," *Appl. Opt.* **24**(9), 1355–1365 (1985).
25. K. V. Gilev et al., "Comparison of the discrete dipole approximation and the discrete source method for simulation of light scattering by red blood cells," *Opt. Express* **18**(6), 5681–5690 (2010).
26. L. Bi and P. Yang, "Modeling of light scattering by biconcave and deformed red blood cells with the invariant imbedding T-matrix method," *J. Biomed. Opt.* **18**(5), 055001 (2013).
27. M. A. Yurkin, "Symmetry relations for the Mueller scattering matrix integrated over the azimuthal angle," *J. Quant. Spectrosc. Radiat. Transf.* **131**, 82–87 (2013).
28. C. F. Bohren and D. R. Huffman, *Absorption and Scattering of Light by Small Particles*, Wiley, New York (1983).
29. M. A. Yurkin et al., "Experimental and theoretical study of light scattering by individual mature red blood cells by use of scanning flow cytometry and a discrete dipole approximation," *Appl. Opt.* **44**(25), 5249–5256 (2005).
30. D. W. Mackowski and M. I. Mishchenko, "A multiple sphere T-matrix Fortran code for use on parallel computer clusters," *J. Quant. Spectrosc. Radiat. Transf.* **112**(13), 2182–2192 (2011).
31. M. A. Yurkin and A. G. Hoekstra, "The discrete-dipole-approximation code ADDA: capabilities and known limitations," *J. Quant. Spectrosc. Radiat. Transf.* **112**(13), 2234–2247 (2011).
32. S. Karpatkin and A. Charmatz, "Heterogeneity of human platelets," *J. Clin. Invest.* **48**(6), 1073–1082 (1969).
33. A. Mathur and J. F. Martin, "Platelet heterogeneity: physiology and pathological consequences," in *Platelets in Thrombosis And Non-Thrombosis Disordorders*, P. Gresele et al., Eds., pp. 70–79, Cambridge University Press, New York (2002).
34. M. M. Frojmovic and R. Panjwani, "Geometry of normal mammalian platelets by quantitative microscopic studies.," *Biophys. J.* **16**(9), 1071–1089 (1976).
35. G. V. Born et al., "Quantification of the morphological reaction of platelets to aggregating agents and of its reversal by aggregation inhibitors," *J. Physiol.* **280**, 193–212 (1978).
36. "LiteBil," 2010, http://albin.abo.fi/~jkniivil/litebil (30 March 2010).
37. G. V. Dyatlov et al., "The scanning flow cytometer modified for measurement of two-dimensional light-scattering pattern of individual particles," *Meas. Sci. Technol.* **19**(1), 015408 (2008).

Alexander E. Moskalensky graduated from the Biomedical Physics Department of Novosibirsk State University in 2012. Currently, he is a PhD student at the Laboratory of Cytometry and Biokinetics in the Institute of Chemical Kinetics and Combustion, Novosibirsk, Russia. His research interests include flow cytometry and simulation of light scattering by biological cells. His degree work is aimed at study of blood platelets shape change and aggregation with the scanning flow cytometry.

Dmitry I. Strokotov graduated from the Biomedical Physics Department of Novosibirsk State University in 2008. Currently, he is a researcher at the Laboratory of Cytometry and Biokinetics in the Institute of Chemical Kinetics and Combustion, Novosibirsk, Russia. He received his PhD degree in biophysics from the Institute of Biophysics, Krasnoyarsk, in 2011. His current research interests are focused on scanning flow cytometry and methods for characterization of biological mononuclear cells.

Andrei V. Chernyshev graduated from the Chemical Physics Department of Novosibirsk State University in 1988. He received his PhD degree from the Institute of Chemical Kinetics and Combustion, Novosibirsk, in 1998. Now, he is a senior research fellow in the Laboratory of Cytometry and Biokinetics in the Institute. His current research interests are cellular physiology and molecular biokinetics.

Valeri P. Maltsev received his PhD degree (1996) and DrSci degree (2001) in biophysics from the Krasnoyarsk State University and from the Institute of Automation and Electrometry, Novosibirsk, Russia, respectively. Now, he is a head of the Biomedical Physics Department in Novosibirsk State University and Laboratory of Cytometry and Biokinetics in Institute of Chemical Kinetics and Combustion, Novosibirsk, Russia. His current research is focused on scanning flow cytometry and methods for characterization of biological cells.

Maxim A. Yurkin is a senior researcher at Institute of Chemical Kinetics and Combustion SB RAS. He holds PhD degrees in computational science from University of Amsterdam and in biophysics from Institute of Chemical Kinetics and Combustion (Novosibirsk). His current research interests include the discrete dipole approximation, inverse light-scattering problems, and characterization of blood cells. He has published over 30 peer-reviewed papers and received young scientist's award in electromagnetic and light scattering by Elsevier.